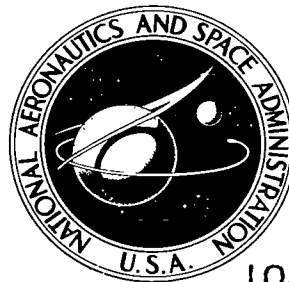


NASA TECHNICAL NOTE



NASA TN D-4514

e.1

NASA TN D-4514

LOAN COPY: R
AFWL (W)
KIRTLAND AFB

0131223



HEAT-TRANSFER CORRELATION FOR GAS FLOW ACROSS HEATED BANKS OF WIRE MESHES OR TUBES

by Byron L. Siegel
Lewis Research Center
Cleveland, Ohio

TECH LIBRARY KAFB, NM



0131223

HEAT-TRANSFER CORRELATION FOR GAS FLOW ACROSS
HEATED BANKS OF WIRE MESHES OR TUBES

By Byron L. Siegel

Lewis Research Center
Cleveland, Ohio

NATIONAL AERONAUTICS AND SPACE ADMINISTRATION

For sale by the Clearinghouse for Federal Scientific and Technical Information
Springfield, Virginia 22151 - CFSTI price \$3.00

HEAT-TRANSFER CORRELATION FOR GAS FLOW ACROSS HEATED BANKS OF WIRE MESHES OR TUBES

by Byron L. Siegel
Lewis Research Center

SUMMARY

The heat-transfer data of this investigation for nitrogen flowing across a bank of electrically heated mesh were compared with the data of other investigators for the flow of hydrogen, nitrogen, helium, and air across single meshes, banks of meshes, and banks of tubes. The data covered the following ranges of variables:

- (1) Porosities from 0.37 to 0.88
- (2) Wire or tube diameters from 0.0076 to 0.375 inch (0.0193 to 0.952 cm)
- (3) Surface temperatures to 5500° R (3050° K)
- (4) Outlet gas temperatures to 3160° R (1760° K)
- (5) Reynolds numbers from 3 to 30 000

A heat-transfer correlation based on surface-temperature gas property evaluation, wire diameter, and average mesh flow area was found which correlated the data within ± 20 percent.

INTRODUCTION

Forced-convection heat-transfer characteristics for flow through wire-mesh heating elements have been reported in reference 1. A heat-transfer correlation of this reference was based on tests of single wire mesh. Operation of the heater of reference 2 with banks of meshes resulted in apparently different heat-transfer characteristics.

In the present investigation, two different mesh banks were tested separately in the gas heater, and heat-transfer data were obtained. The purpose of this investigation was to find a correlation for the mesh-bank data of this study. Such a correlation was formulated by using the data of various other investigators. These include data on wire-mesh banks and tube banks (refs. 3 to 5) obtained by a transient technique at low temperatures where variations in fluid properties are so small as to be neglected, as well

as data on single wire mesh and tube banks (refs. 6 to 8) obtained in steady-state tests at higher temperatures where fluid-property variations are large and cannot be neglected.

The end result was a correlation for all these data, including the data of this investigation within about ± 20 percent. These data cover mesh porosities from 0.37 to 0.88, wire or tube diameters from 0.0076 to 0.375 inch (0.0193 to 0.952 cm), surface temperatures up to 5500° R (3050° K), outlet gas temperatures up to 3160° R (1760° K), and Reynolds numbers from 3 to 30 000.

APPARATUS AND PROCEDURE

Heat-transfer data were obtained for forced flow of nitrogen across a bank of tungsten wire meshes by using the hot gas heater facility of reference 2. A general description of the facility is presented here; however, a more detailed description can be found in reference 2. The hot gas heater is comprised of four banks of tungsten mesh elements. Only the last bank of the heater was used to obtain the data of this investigation, and this bank was operated with six and eight meshes.

The flow system, test section, and instrumentation associated with this heater are shown schematically in figure 1. A description of these components and of the heater used in this investigation is given under the corresponding subheadings.

Test Section

Figure 2 shows the heater bank used as the test section for this investigation. All four banks of the heater are identical to the one shown in figure 2. The heater bank is composed of two water-cooled copper buses, two molybdenum buses, two boron nitride housings, and a bank of six or eight single-mesh heating elements with associated molybdenum clamping wedges and bolts.

The mesh is formed by interwound helical coils of tungsten wire. The coil ends are sandwiched between two tungsten plates approximately 0.060 inch (0.1525 cm) thick. The ends of the coils are heliarc welded to the plates to provide positive electrical connections. The mesh elements are clamped between the molybdenum buses by the clamping wedge arrangement shown in figure 2.

Water-cooled copper buses are bolted to the back side of the molybdenum buses with molybdenum bolts, the heads of which are recessed in counterbored holes within the copper buses and can be seen in figure 2. The gas flow passage is formed by the walls of the molybdenum buses on two sides and the boron nitride electrical insulating pieces

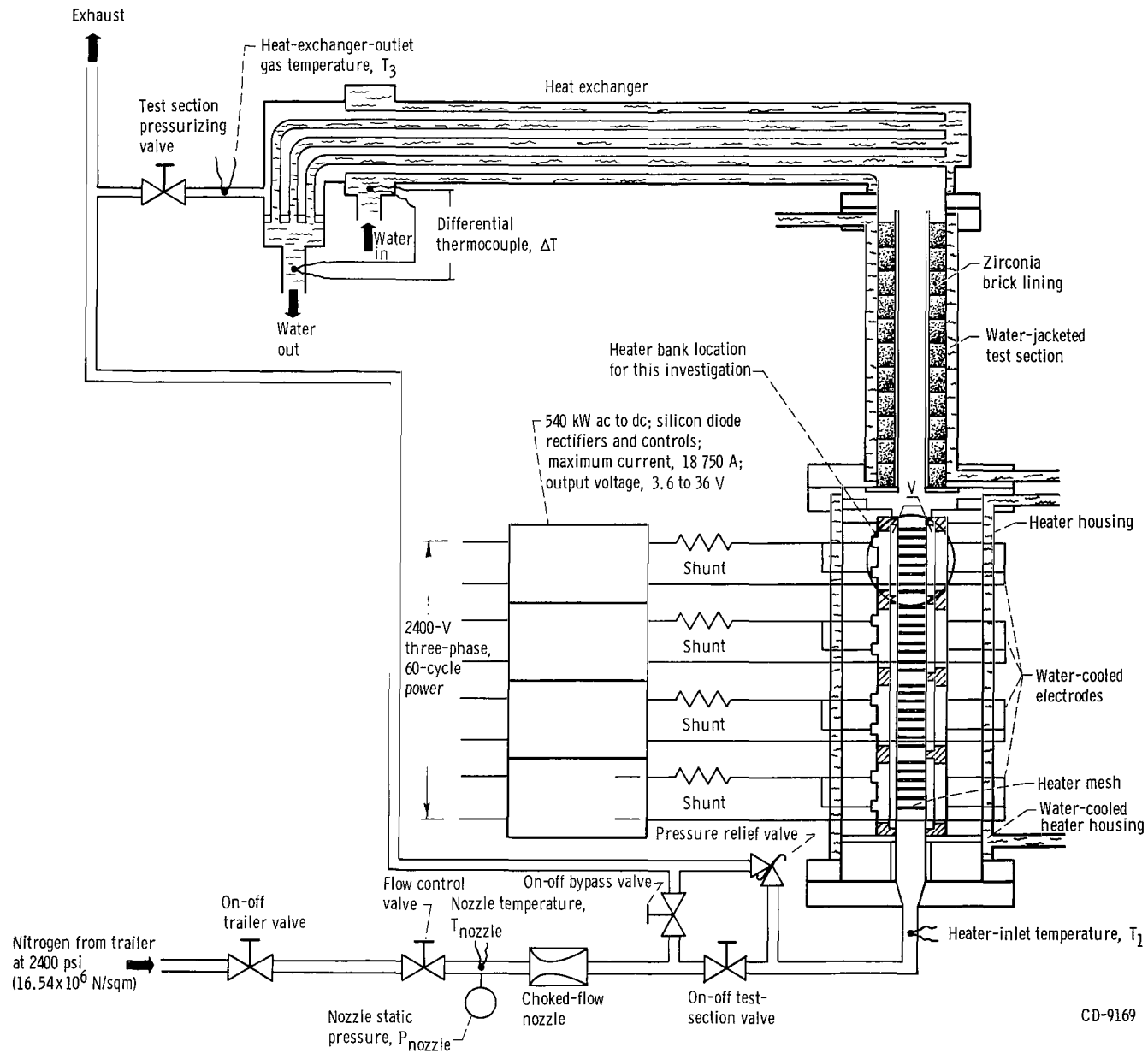
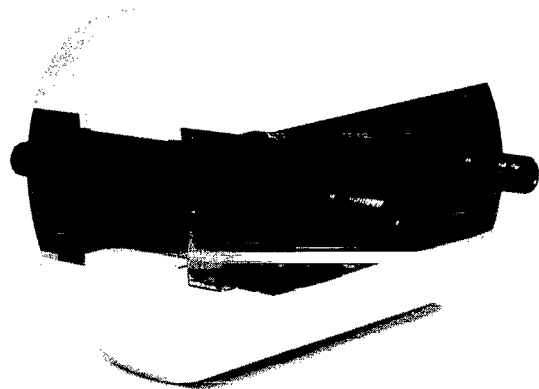
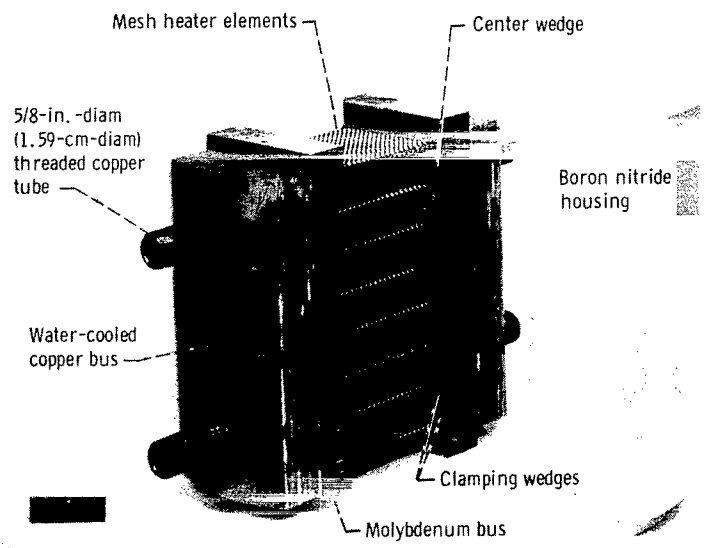


Figure 1. - Flow system, test section, and instrumentation.



C-66-4225



C-66-4226

Figure 2. - Heater bank and components.

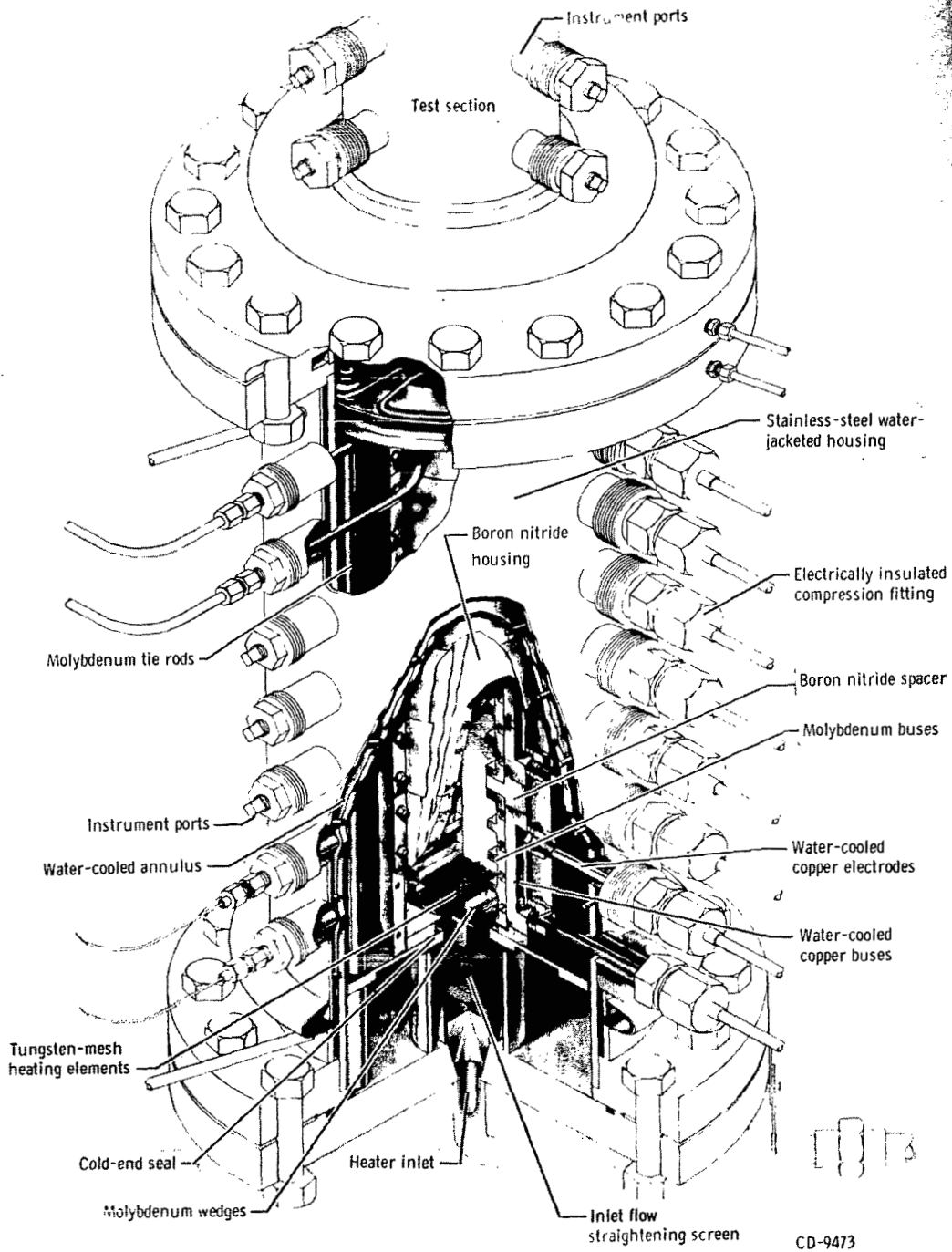


Figure 3. - Heater assembly with cutaway views of hot end and mesh bank assembly.

on the other two sides. The outside surfaces of both the boron nitride housings and the water-cooled copper buses have the same radius of curvature and form a complete cylinder having a 3-inch (7.62-cm) radius, as shown in figure 2. Except for the 1/64-inch (0.040-cm) clearance between the mesh and the boron nitride side walls on each side, the mesh heating elements completely fill the 2- by 2 $\frac{1}{8}$ -inch (5.08- by 5.4-cm) rectangular flow channel formed by the busing and boron nitride.

The heater bank is contained in a water-jacketed, stainless-steel housing shown in the cutaway isometric view of the heater in figure 3. Water-cooled electrodes connect the heater to the existing busing located outside the housing.

Flow System

As may be seen in figure 1, nitrogen is supplied to the flow system from a tube trailer at a maximum pressure of 2400 pounds per square inch (16.54×10^6 N/m²). From the trailer, the gas flows through a remotely operated, pressure-regulating control valve, a choked-flow nozzle, and an on-off valve that supplies gas directly to the heater. Three interchangeable nozzles are available to cover a range of flow rates from 0.02 to 1 pound per second (0.00907 to 0.454 kg/sec).

From the heater, the hot gas flows through a water-cooled, test-section housing, which is lined with zirconia fire brick, and into a gas-to-water tube and shell heat exchanger, where it is cooled before it is exhausted into the atmosphere. The gas passes through the heat exchanger between the water-cooled tubes and water-jacketed shell and then into the exhaust stack to the atmosphere. A remotely operated, back-pressure valve is located downstream of the heat exchanger for pressurizing the test section during operation or for pressure checking prior to operation.

There are two water flow systems associated with this facility: (1) a cooling-tower water system which is used to cool the water-jacketed housings, flanges, and heat exchanger; and (2) a city water supply which is used to cool the buses that bring electrical power from the power supplies to the heater. Because of the size of conventional busing that would be required to carry the current (as high as 18 750 amps) from the power supply terminals to the heater, water-cooled busing was used.

Instrumentation

The instrumentation used is shown in figure 1. The current flowing through the heater bank was measured by a calibrated shunt having a 1-millivolt drop per 400 amperes. The test-section voltage was measured between the tungsten end plates of the

mesh heating elements by a digital voltmeter.

The heater outlet gas temperature was calculated from the heat picked up by the water in the heat exchanger plus the residual heat that remains in the gas that leaves the heat exchanger. The flow rate of the water in the heat exchanger was measured by a calibrated orifice, and the temperature rise of the water was measured by a differential iron-Constantan thermocouple. This method was used instead of a direct thermocouple reading to determine the heater outlet gas temperature because of the difficulty in installing a thermocouple at the heater exit and in obtaining a mixed bulk gas temperature. The accuracy of a calculated gas temperature, based on the use of the heat exchanger as a calorimeter, has been checked in the past against temperature readings obtained with thermocouples, melting plugs, and optical measurements and has proved to be in good agreement with these other methods. Measurements of the heat loss from the gas in passing through the water-jacketed test section showed this loss to be negligible. Heater inlet gas temperature and heat exchanger exhaust gas temperature were measured by type-K thermocouples (designation of ref. 9).

A choked-flow nozzle was used to measure gas flow rates. The gas flow rate was set by adjusting the nozzle inlet pressure. Constant gas flow was maintained provided the exit pressure was not raised too high to unchoke the nozzle.

The nozzle inlet pressure was measured by a temperature-compensated strain gage bridge pressure transducer. All temperatures and currents were continuously recorded on null-balance potentiometer-type recorders.

METHOD OF CALCULATION

Average Heat-Transfer Coefficients

The average heat-transfer coefficient for the mesh bank was computed from the experimental data by the relation

$$h = \frac{Q}{A_s \left(T_s - \frac{T_1 + T_2}{2} \right)} \quad (1)$$

All symbols are defined in the appendix. The outlet gas temperature from the heater T_2 and the heat input to the gas Q were determined from a heat balance on the heat exchanger.

The heat input to the gas Q can be calculated from the sum of heat picked up by the

water in the heat exchanger and the residual heat remaining in the gas leaving the heat exchanger:

$$Q = W_1 c_{p, w} \Delta T + W c_{p, e} (T_3 - T_1) \quad (2)$$

The temperature of the gas entering the heat exchanger is assumed to be the same as that leaving the heater. This assumption is justified because the heat picked up in the water flowing through the test-section water jacket was negligible because of the good thermal insulating properties of the zirconia fire bricks. By equating the right side of equation (2) to the heat picked up by the gas $W c_{p, h} (T_2 - T_1)$, the outlet gas temperature T_2 can be calculated as follows:

$$T_2 = \frac{W_1 c_{p, w} \Delta T + W c_{p, e} (T_3 - T_1)}{W c_{p, h}} + T_1 \quad (3)$$

The nitrogen properties used were taken from reference 10. The determinations of T_s and A_s in equation (1) are discussed in the following section.

Geometrical Factors

The mesh heating elements are made of interwound helical tungsten coils. These meshes can be completely specified by the following five parameters: (1) wire diameter d , (2) mandrel diameter D , (3) number of parallel coils per mesh N , (4) length of mesh b , and (5) helical coil pitch p .

The wire length of a single helical coil S is given by the equation

$$S = \frac{b}{p} \sqrt{\pi^2 (D + d)^2 + p^2} \quad (4)$$

The total heat-transfer surface area for N number of coils is

$$A_s = \pi d S N \quad (5)$$

The equivalent diameter for porous media is normally defined as

$$D_e = \frac{4(\text{Void volume})}{A_s} = \frac{4LA_{fl}}{A_s} \quad (6)$$

where the average flow area is given as

$$A_{fl} = \epsilon A_{ft} \quad (7)$$

The porosity is defined as the average porosity for the entire mesh volume by

$$\epsilon = \frac{\text{Void volume}}{\text{Volume of mesh}} \quad (8)$$

The porosity for tube banks is determined in the same manner.

The average surface temperature of the mesh was determined from the relation between temperature and resistivity of tungsten as given in reference 11. The resistivity was calculated by the equation

$$\zeta = \frac{V}{I} \frac{A}{S} \quad (9)$$

where A is the current flow cross sectional area of the wire mesh bank for N^* number of meshes and equals

$$A = \frac{N^* N \pi d^2}{4} \quad (10)$$

The mesh geometrical parameters are given in table I.

TABLE I. - MESH GEOMETRIC PARAMETERS FOR HEATER BANK

Parameter	Mesh bank	
	1	2
Wire diameter, d , in. (cm)	0.0350 (0.0888)	0.0300 (0.0762)
Mandrel diameter, D , in. (cm)	0.0800 (0.203)	0.0800 (0.203)
Equivalent diameter, D_e , in. (cm)	0.0650 (0.164)	0.071 (0.1805)
Mesh length, b , in. (cm)	2.125 (5.4)	2.125 (5.4)
Mesh width, w , in. (cm)	2 (5.08)	2 (5.08)
Number of parallel coils per mesh, N	36	36
Coil pitch, p , in./turn (cm/turn)	0.125 (0.317)	0.111 (0.282)
Porosity, ϵ	0.65	0.703
Number of meshes per bank, N^*	8	6

RESULTS AND DISCUSSION

The heat-transfer data for the banks of wire meshes of table I are presented in table II. These data were obtained with forced flow of nitrogen through six and eight meshes per bank as indicated in the tables. Nusselt, Prandtl, and Reynolds numbers were calculated from these data by using fluid properties evaluated at bulk or surface temperature. Also, values of Reynolds number were calculated by using characteristic lengths of equivalent diameter D_e or wire diameter d and mass velocities based on frontal area or average flow area. The heat-transfer coefficient used in the Nusselt number is an average value for the entire bank, as discussed in the section METHOD OF CALCULATION.

Heat-transfer data for single wire meshes have been correlated in reference 1 by the following equation:

$$\frac{hD_e/k_s}{Pr_s^{0.4}} = 0.462 \left(\frac{GD_e}{\mu_s} \right)^{0.53} \quad (11)$$

where D_e is the equivalent diameter and G is the mass velocity based on the average flow area.

Figure 4 shows a plot of the data of this investigation based on the above correlation. The data fall considerably higher than the solid line representing equation (11). Furthermore, in figure 4 the slopes of the data at different flow rates are almost parallel to each other but different from the curve of equation (11). Obviously, equation (11) does not correlate the data of this investigation. This may be attributed initially to either the fact that single meshes have different heat-transfer characteristics than banks of meshes, or the fact that the test conditions for this investigation are substantially different from those of reference 1. In regard to the test conditions, it is worth noting that the surface-to-bulk temperature ratio varies from mesh to mesh as the fluid passes through a bank of meshes. Thus, a single data point for a bank of meshes (average heat-transfer coefficient) involves a wide range in surface-to-bulk temperature ratios.

Heat-transfer data for banks of meshes and banks of tubes were correlated in reference 6 by the following equation:

$$\frac{hd/k_b}{Pr_b^{0.4}} = 0.75 \left(\frac{G_{ft}d}{\mu_b} \right)^{0.52} \quad (12)$$

TABLE II. - MESH BANK HEAT-TRANSFER DATA

[Gas, nitrogen.]

Test	Voltage, V	Current, I, amperes	Average surface temperature, T _s		Outlet gas temperature, T ₂		Gas flow rate, W	
							lb/sec	kg/sec
			°R	°K	°R	°K		
Mesh bank 1; inlet gas temperature, 540° R (300° K)								
1	3.34	12 200	1980	1100	2310	1280	0.0762	0.0345
2	4.22	12 650	2340	1300	2630	1460	↓	↓
3	5.16	13 100	2690	1490	2960	1640	↓	↓
4	3.55	11 300	2220	1230	2650	1470	.0548	.0248
5	4.83	11 800	2780	1540	3160	1760	.0548	.0248
6	4.05	14 750	1980	1100	2200	1220	.1232	.0558
7	5.26	15 350	2390	1330	2570	1430	↓	↓
8	7.02	16 100	2930	1630	3130	1740	↓	↓
9	4.36	16 200	1950	1080	2080	1150	.1605	.0728
10	5.86	17 000	2410	1340	2520	1400	↓	↓
11	7.37	17 500	2850	1580	2920	1620	↓	↓
Mesh bank 2; inlet gas temperature, 530° R (294° K)								
1	2.05	8 700	990	550	870	483	0.233	0.106
2	3.84	10 500	1440	800	1230	684	↓	↓
3	5.8	11 000	1960	1090	1580	878	↓	↓
4	7.75	11 400	2430	1350	1880	1040	↓	↓
5	9.72	11 700	2880	1600	2190	1220	↓	↓
6	3.64	12 700	1170	650	920	511	.4710	.213
7	5.55	13 600	1580	878	1160	644	↓	↓
8	7.53	14 100	1980	1100	1390	771	↓	↓
9	9.58	14 400	2380	1320	1570	872	↓	↓
10	11.45	14 700	2720	1510	1750	972	↓	↓
11	3.53	14 000	1050	583	820	455	.688	.314
12	5.39	15 300	1390	772	970	538	↓	↓
13	7.33	15 900	1750	972	1140	634	↓	↓
14	9.32	16 200	2110	1170	1300	722	↓	↓
15	11.28	16 500	2440	1360	1480	822	↓	↓
16	13.44	16 900	2770	1540	1660	922	↓	↓
17	9.28	16 500	2070	1150	1410	784	.756	.343
18	11.24	16 900	2380	1320	1530	850	↓	↓
19	13.24	17 100	2710	1500	1590	883	↓	↓
20	14.21	17 200	2860	1590	1650	916	↓	↓
21	15.17	17 400	3000	1670	1700	944	↓	↓
22	16.16	17 500	3150	1750	1830	1020	↓	↓
23	17.15	17 600	3290	1830	1900	1050	↓	↓
24	18.13	17 800	3420	1900	1950	1080	↓	↓
25	19.12	17 900	3560	1980	2030	1130	↓	↓

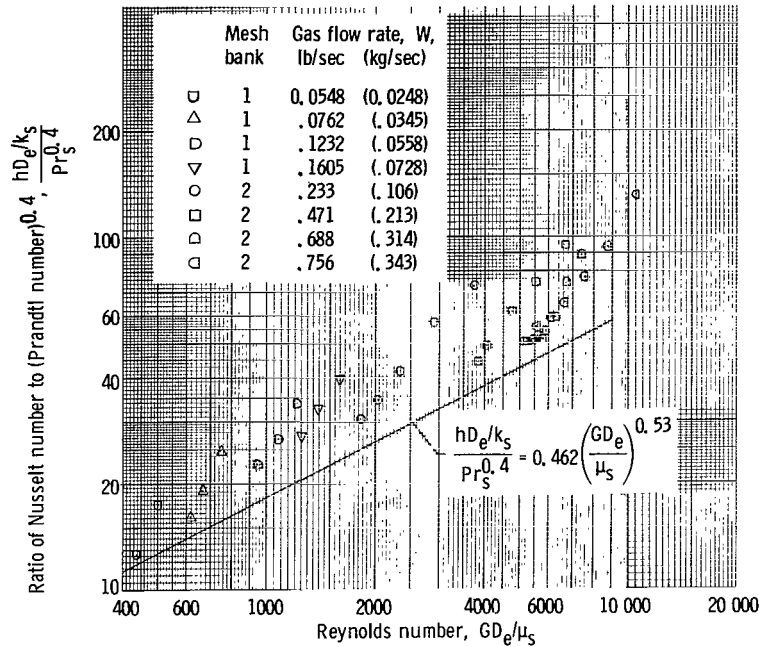


Figure 4. - Heat-transfer data of this investigation plotted on basis of correlation reported in reference 1.

where d is the wire diameter and G_{ft} is the mass velocity based on frontal area. By using equation (12), reference 6 showed good agreement between the data of reference 3 for woven mesh matrices and the data of reference 7 for tube banks. However, the present analysis revealed that a better correlation can be achieved for both tube and mesh banks if the mass velocity in the Reynolds number is based on the average flow area. Considering only transient data from references 3 to 5, the effect of fluid-property variations can be minimized because these data were all obtained at low temperatures. The transient data for tube and mesh banks are plotted in figure 5, where the Reynolds number is expressed in terms of wire diameter and mass velocity based on average flow area. The data fall on a slightly curved line on log-log paper and can be represented by two straight lines according to the following equations:

$$\frac{hd/k_b}{Pr_b^{0.4}} = 0.55 \left(\frac{Gd}{\mu_b} \right)^{0.56} \quad \left(\text{for } \frac{Gd}{\mu_b} \text{ from 3 to 1000} \right) \quad (13)$$

$$\frac{hd/k_b}{Pr_b^{0.4}} = 0.32 \left(\frac{Gd}{\mu_b} \right)^{0.64} \quad \left(\text{for } \frac{Gd}{\mu_b} \text{ from 1 000 to 30 000} \right) \quad (14)$$

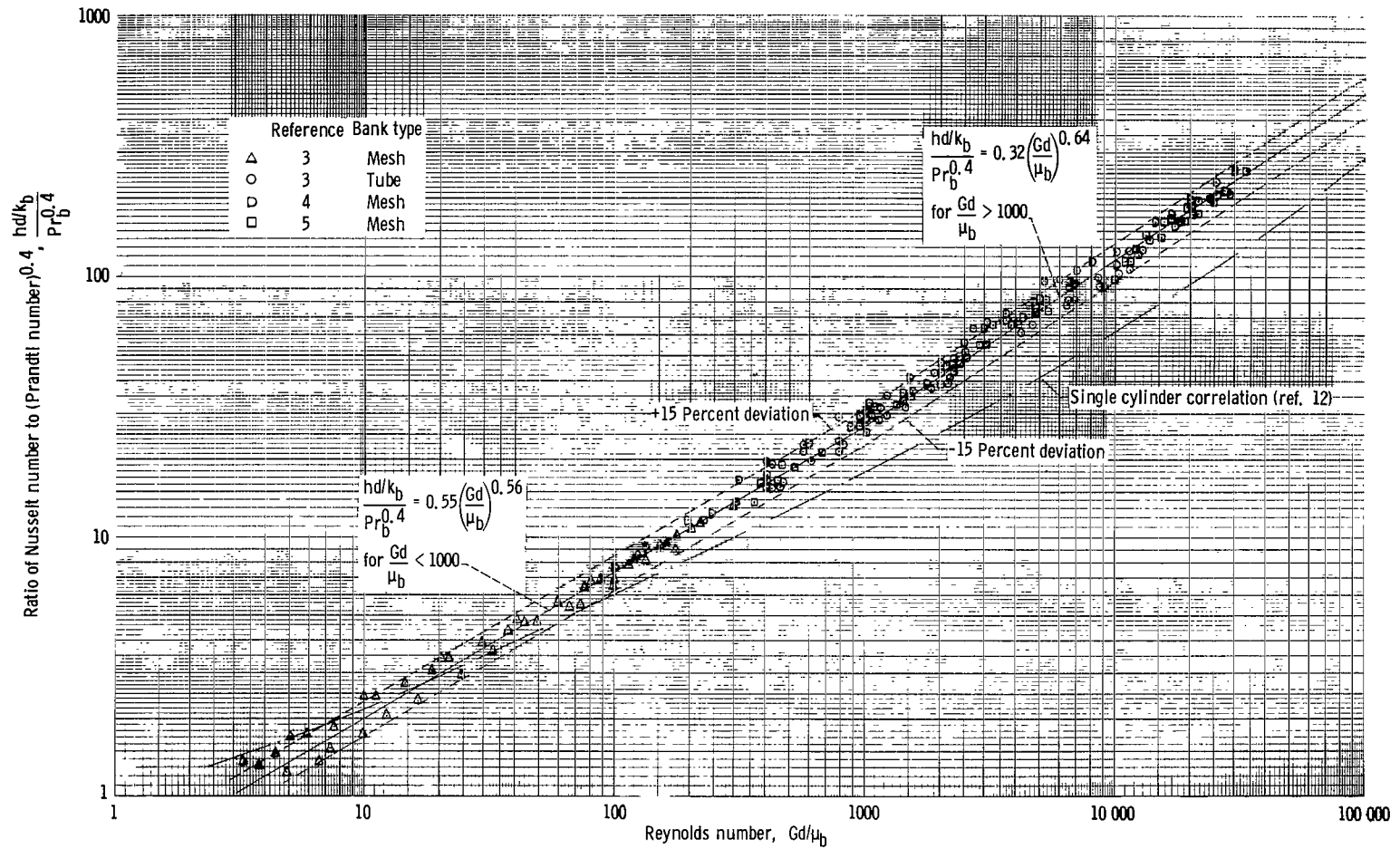


Figure 5. - Heat-transfer correlation based on data of other investigators for convective heat transfer over banks of meshes and tubes obtained by transient techniques. Bulk properties; d wire diameter; G evaluated at average cross sectional flow area.

Two dashed lines representing ± 15 percent deviation are also shown in figure 5. The use of average flow area instead of frontal area results in a better correlation, and the average flow area is probably a more representative geometrical parameter in evaluating Reynolds number, especially for lower porosity geometries.

All the data presented in figure 5 were obtained by a low-temperature, transient technique where variation in fluid properties with temperature is negligible; hereinafter, these data are referred to as transient data. The data of reference 4 are for air flow across random, in-line and staggered banks of cross-rod mesh matrices. The data of reference 5 are for air flow across woven and cross-rod matrices. Also included in figure 5 are the data of reference 3 for air flow normal to banks of various staggered and in-line bare tube arrangements. Table III gives the range of the variables covered by the data of references 3 to 5. The calculated porosities are based on a single row of meshes or tubes, and separation between adjacent rows is not considered in the calculation. Reference 3 shows little or no difference in heat-transfer coefficient between packed or separated banks of meshes.

Excellent agreement was obtained for the transient data of all investigators presented in figure 5. The dashed lines shown represent ± 15 percent deviation for the correlating lines. The dot-dash line in figure 5 represents the single-cylinder correlating line of reference 12. With increasing Reynolds number, the data fall progressively higher relative to the single-cylinder correlating line. This result can be attributed to the additional turbulence promoted by adjacent wires which results in an increase in heat transfer. At low Reynolds numbers there is more scatter in the data, and a majority of the points fall below the single-cylinder correlating line. This pattern is attributed to the total mesh heat-transfer surface area being used to evaluate the heat-transfer coefficient. An effective surface area which excludes the overlapping wire mesh surface should be used. Unfortunately, a means of evaluating the effective surface areas of the complex geometries involved in this investigation has not been determined. At high Reynolds numbers the effect of using the total heat-transfer surface area is secondary in comparison to the increase in turbulence promoted by adjacent wires or tubes.

It can be concluded from figure 5 that a correlation for both banks of meshes and tubes covering a variety of geometric configurations and porosities has been obtained for constant properties.

The data of the present investigation are plotted on the same basis as the correlation for the transient data of figure 5. These present data, along with the two correlating lines representing equations (13) and (14), are shown in figure 6. These data fall below the correlating lines and show about the same flow dependency as that exhibited in figure 4.

TABLE III. - RANGES OF VARIABLES COVERED BY REFERENCES USED

Refer- ence	Geometry	Porosity	Tube or wire diameter, d		Surface temperature, T _s		Outlet gas temperature, T ₂		Modified Reynolds number, $\frac{Gd}{\mu_s} \frac{T_b}{T_s}$
			in.	cm	°R	°K	°R	°K	
1	Single mesh	0.64 to 0.722	0.020 to 0.035	0.0508 to 0.089	920 to 5200	510 to 2890	645 to 2400	358 to 1330	35 to 490
6	Single mesh	0.727 to 0.884	0.030 to 0.050	0.076 to 0.127	1523 to 5500	846 to 3050	655 to 3020	363 to 1680	15 to 225
3	Tube banks	0.372 to 0.608	0.250 to 0.375	0.635 to 0.952	(a)	(a)	(a)	(a)	^b 402 to 12 860
	Mesh banks	0.602 to 0.832	0.0076 to 0.041	0.0193 to 0.104	(a)	(a)	(a)	(a)	^b 3 to 296
7	Tube bank	0.602	0.020	0.0508	683 to 1109	379 to 616	598 to 946	332 to 526	62 to 1010
4	Cross rod matrices	0.5 to 0.832	0.375	0.952	(a)	(a)	(a)	(a)	^b 95 to 30 000
5	Cross rod matrices	0.602 to 0.832	0.375	0.952	(a)	(a)	(a)	(a)	^b 303 to 33 600
8	Tube banks	0.372 to 0.74	0.31	0.786	710 to 1210	394 to 672	600 to 910	330 to 505	1615 to 24 500
This report	Mesh banks	0.65 to 0.703	0.030 to 0.035	0.0762 to 0.089	990 to 3560	550 to 1980	820 to 3160	455 to 1760	156 to 2873

^aLow-temperature transient data.

^bValue of T_b/T_s is approximately 1 for transient data.

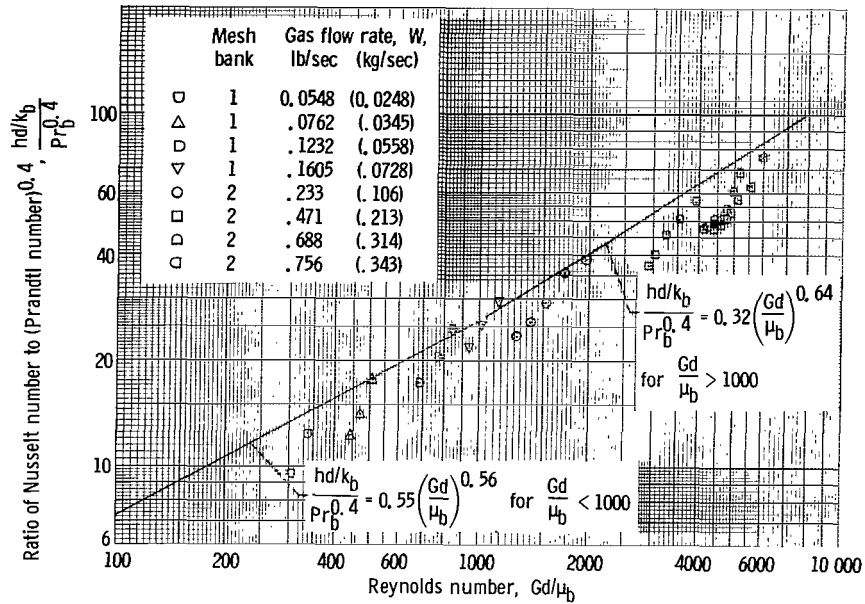


Figure 6. - Comparison of heat-transfer data of this investigation and heat-transfer correlation lines obtained by using transient data of other investigators.

To bring the data closer to the correlating lines, a variable property correlation reported in reference 13 was used. The best results were obtained by using a modified Reynolds number with fluid properties evaluated at surface temperatures. On this basis, equations (13) and (14) become

$$\frac{hd/k_s}{Pr_s^{0.4}} = 0.55 \left(\frac{Gd}{\mu_s} \frac{T_b}{T_s} \right)^{0.56} \quad \left(\text{for } \frac{Gd}{\mu_s} \frac{T_b}{T_s} \text{ from 3 to 1000} \right) \quad (15)$$

$$\frac{hd/k_s}{Pr_s^{0.4}} = 0.32 \left(\frac{Gd}{\mu_s} \frac{T_b}{T_s} \right)^{0.64} \quad \left(\text{for } \frac{Gd}{\mu_s} \frac{T_b}{T_s} \text{ from 1 000 to 30 000} \right) \quad (16)$$

where $(Gd/\mu_s)(T_b/T_s)$ is a modified Reynolds number with gas properties evaluated at surface temperature. Average flow area and wire diameter are still used as the geometrical parameters. The results are shown in figure 7, where this modified Reynolds number is plotted against the ratio of Nusselt to Prandtl number to the 0.4 power. The lines representing equations (15) and (16) are also shown in figure 7. The data of this

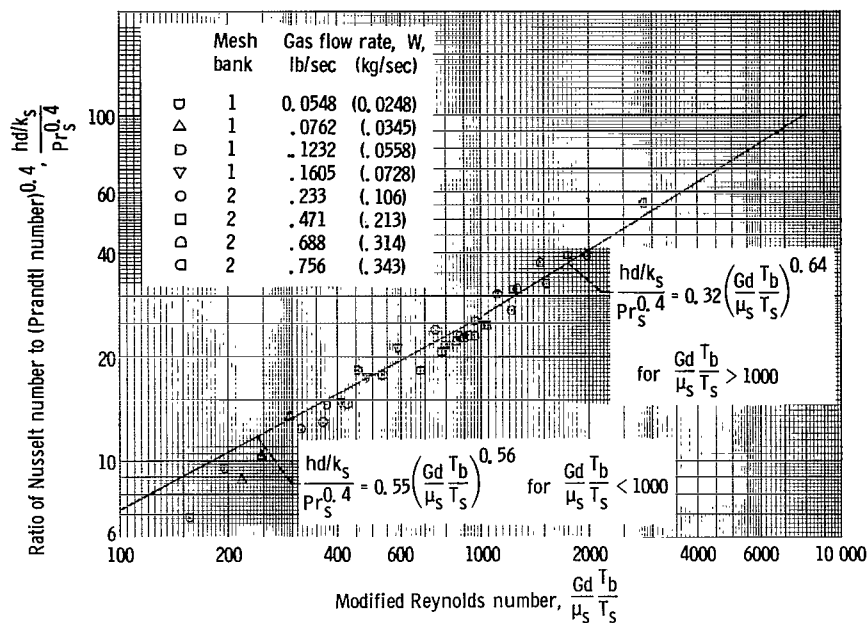


Figure 7. - Plot of data of this investigation with use of modified Reynolds number correlation with fluid properties evaluated at surface temperatures.

investigation are in good agreement with the correlating lines, and most of the flow and temperature dependency exhibited in figures 4 and 6 has been eliminated by use of this modified surface temperature correlation. Because the transient data represented by equations (13) and (14) have small temperature variations, equations (15) and (16) can also be used to represent these data.

The data of references 1, 6, 7, and 8, as well as the correlating lines representing equations (15) and (16), are shown in figure 8. Table III gives the range of variables covered by the data of each of these references. The data of these investigators were all obtained under steady-state conditions. In reference 8, the data were evaluated at film-temperature properties, and a tabulation of the data was not available. However, surface and gas temperatures were sufficiently low (maximum surface temperature, 1210°R (672°K); maximum gas temperature, 910°R (505°K)) so that converting from film to surface properties would involve minor corrections. The data of reference 1 are for flow of nitrogen and hydrogen across single meshes of the same geometry as those of this investigation. The data of reference 6 are for flow of nitrogen, hydrogen, and helium across single meshes of helical tungsten wires located side by side but not interwound. The data of reference 7 are for flow of air across banks of electrically heated rods. Representative points were taken from the curves of reference 8 for flow of air across various tube bank arrangements. The correlating lines of equations (15) and (16)

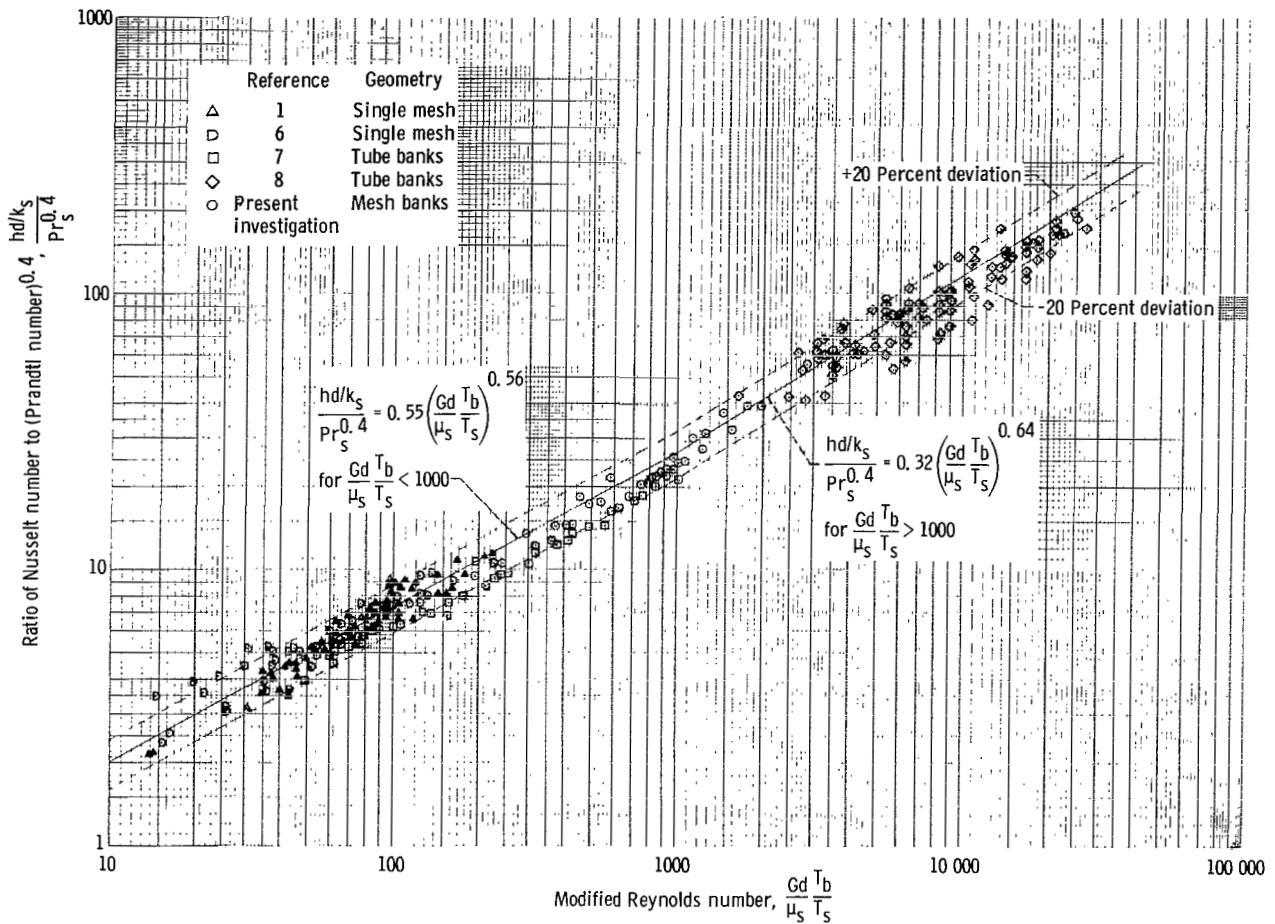


Figure 8. - Data of this investigation and nontransient data of other investigators plotted by using modified Reynolds number correlation with fluid properties evaluated at surface temperatures.

and two pairs of dashed lines representing ± 20 percent deviation from the correlation are also shown in figure 8.

More than 90 percent of the data points of references 1 and 6 for single meshes are within ± 20 percent of the correlating line; this indicates that the correlation is valid for individual meshes, as well as for banks of meshes and tubes. Although the data of reference 8 have more scatter than the data of the other references reported, they were included in figure 8 because they extended the range of Reynolds number over which the correlation is valid. Over 80 percent of these data are within ± 20 percent, and 98 percent of these data are within ± 30 percent of the correlating lines. Thirty-eight tube arrangements are covered in reference 8, and most of the scatter can be attributed to only four of these arrangements. The data shown in figure 8 cover a Reynolds number range from 13 to 28 000 for air, hydrogen, nitrogen, and helium flowing across meshes and tube banks having porosities between 0.37 and 0.88.

Since the low-temperature transient data of figure 5 are unaffected by the use of bulk, film, or surface properties, they could be plotted on the basis of figure 8, and they would plot essentially the same as in figure 5. Therefore, equations (15) and (16) correlate all the data presented herein over a range of Reynolds number from 3 to 30 000.

SUMMARY OF RESULTS

Forced convective heat-transfer data were obtained for nitrogen flow across electrically heated banks of six or eight tungsten wire meshes. These data were compared with the low-temperature data of other investigators for the flow of air across banks of tubes and meshes, as well as with the high-temperature data for the flow of nitrogen, hydrogen, and helium across single wire mesh surfaces. The data used covered the following ranges of variables: porosities from 0.37 to 0.88, wire or tube diameters from 0.0076 to 0.375 inch (0.0193 to 0.952 cm), surface temperatures to 5500° R (3050° K), outlet gas temperatures to 3160° R (1760° K), and Reynolds numbers from 3 to 30 000.

A forced convection, heat-transfer correlation valid for various single-mesh, mesh-bank, and tube-bank arrangements was obtained. This correlation is expressed by the following equations, which correlate the data within ±20 percent.

$$\frac{hd/k_s}{Pr_s^{0.4}} = 0.55 \left(\frac{Gd}{\mu_s} \frac{T_b}{T_s} \right)^{0.56} \quad \left(\text{for } \frac{Gd}{\mu_s} \frac{T_b}{T_s} \text{ from 3 to 1000} \right)$$

$$\frac{hd/k_s}{Pr_s^{0.4}} = 0.32 \left(\frac{Gd}{\mu_s} \frac{T_b}{T_s} \right)^{0.64} \quad \left(\text{for } \frac{Gd}{\mu_s} \frac{T_b}{T_s} \text{ from 1 000 to 30 000} \right)$$

where h is the average heat-transfer coefficient of the gas, d is the wire diameter, k_s is the thermal conductivity of the gas evaluated at the surface temperature, Pr_s is the Prandtl number evaluated at the surface temperature, G is the mass velocity across the mesh based on average cross-sectional flow area, μ_s is the absolute viscosity of the gas evaluated at the surface temperature, T_b is the average temperature of the gas in the tube or mesh bank, and T_s is the tube or mesh bank average surface temperature.

Lewis Research Center,
National Aeronautics and Space Administration,
Cleveland, Ohio, November 14, 1967,
120-27-04-56-22.

APPENDIX - SYMBOLS

A	current flow cross-sectional area of mesh bank, sq ft (sq m)
A_{fl}	average cross-sectional flow area of mesh, sq ft (sq m)
A_{ft}	frontal area, sq ft (sq m)
A_s	surface area, sq ft (sq m)
b	length of mesh, ft (m)
c_p	specific heat of gas at constant pressure, Btu/(lb)($^{\circ}$ R) (J/(kg)($^{\circ}$ K))
$c_{p, e}$	average specific heat of residual gas at constant pressure, Btu/(lb)($^{\circ}$ R) (J/(kg)($^{\circ}$ K))
$c_{p, h}$	average specific heat of gas in heater at constant pressure, Btu/(lb)($^{\circ}$ R) (J/(kg)($^{\circ}$ K))
$c_{p, w}$	specific heat of water at constant pressure, Btu/(lb)($^{\circ}$ R) (J/(kg)($^{\circ}$ K))
D	mandrel diameter, ft (m)
D_e	equivalent diameter, ft (m)
d	wire diameter, ft (m)
G	mass velocity across mesh based on average cross-sectional flow area, W/A_{fl} , lb/(sec)(sq ft) (kg/(sec)(sq m))
G_{ft}	mass velocity across mesh based on frontal area, W/A_{ft} , lb/(sec)(sq ft) (kg/(sec)(sq m))
h	average heat-transfer coefficient of gas, Btu/(sec)(sq ft)($^{\circ}$ R) (J/(sec)(sq m)($^{\circ}$ K))
I	current, amperes
k	thermal conductivity of gas, Btu/(ft)(sec)($^{\circ}$ R) (J/(m)(sec)($^{\circ}$ K))
L	thickness of mesh in flow direction, ft (m)
N	number of parallel coils per mesh
N'	number of meshes per bank
P_{nozzle}	nozzle pressure, lb/sq ft (N/sq m)
Pr	Prandtl number, $c_p\mu/k$
p	coil pitch, ft/turn (m/turn)
Q	heat transfer to gas, Btu/sec (J/sec)

S total wire length of single helical coil, ft (m)
T_b average temperature of gas in mesh bank, $(T_1 + T_2)/2$, °R (°K)
T_s mesh bank average surface temperature, °R (°K)
T₁ heater inlet gas temperature, °R (°K)
T₂ heater outlet gas temperature, °R (°K)
T₃ heat exchanger outlet gas temperature, °R (°K)
ΔT temperature rise of water in heat exchanger, °R (°K)
V voltage drop across test section, volts
W gas flow rate, lb/sec (kg/sec)
W₁ heat exchanger water flow rate, lb/sec (kg/sec)
w width of mesh, ft (m)
ε mesh porosity
ξ resistivity of tungsten, (ohm)(ft) ((ohm)(m))
μ absolute viscosity of gas, lb/(sec)(ft) (kg/(sec)(m))

Subscripts:

b bulk
s surface

REFERENCES

1. Siegel, Byron L. ; Maag, William L. ; Slaby, Jack G. ; and Mattson, William F. : Heat-Transfer and Pressure Drop Correlations for Hydrogen and Nitrogen Flowing Through Tungsten Wire Mesh at Temperatures to 5200^o R. NASA TN D-2924, 1965.
2. Siegel, Byron L. : Design and Operation of a High-Temperature Tungsten-Mesh Gas Heater. NASA TM X-1466, 1967.
3. Kays, W. M. ; and London, A. L. : Compact Heat Exchangers. The National Press, 1955.
4. London, A. L. ; Mitchell, J. W. ; and Sutherland, W. A. : Heat-Transfer and Flow-Friction Characteristics of Crossed-Rod Matrices. J. Heat Transfer, vol. 82, no. 3, Aug. 1960, pp. 199-213.
5. Tong, L. S. ; and London, A. L. : Heat-Transfer and Flow-Friction Characteristics of Woven-Screen and Crossed-Rod Matrices. Trans. ASME, vol. 79, no. 7, Oct. 1957, pp. 1558-1570.
6. Maag, William L. ; and Mattson, William F. : Forced-Convection Heat-Transfer Correlation for Gases Flowing Through Wire Mesh at Surface Temperatures to 5500^o R. NASA TN D-3956, 1967.
7. Gedeon, Louis; and Grele, Milton D. : Forced-Convection Heat-Transfer and Pressure-Drop Characteristics of a Closely Spaced Wire Matrix. NACA RM E54D12, 1954.
8. Pierson, Orville L. : Experimental Investigation of the Influence of Tube Arrangement on Convective Heat Transfer and Flow Resistance in Cross Flow of Gases over Tube Banks. Trans. ASME, vol. 59, no. 7, Oct. 1937, pp. 563-572.
9. Anon: Thermocouples and Thermocouple Extension Wires. Rev. Composite RPI. 9-PFI. 7, Instr. Soc. Am. , July 1959.
10. Hilsenrath, Joseph, et al. : Tables of Thermal Properties of Gases. Circular 564, National Bureau of Standards, Nov. 1, 1955.
11. Anon. : Handbook of Chemistry and Physics. Thirty Seventh ed. , Chemical Rubber Publishing Co. , 1956, p. 2360.
12. McAdams, William H. : Heat Transmission. Third ed. , McGraw-Hill Book Company, Inc. , 1954.

13. Humble, Leroy V. ; Lowdermilk, Warren H. ; and Desmon, Leland G. : Measurements of Average Heat-Transfer and Friction Coefficients for Subsonic Flow of Air in Smooth Tubes at High Surface and Fluid Temperatures. NACA TR-1020, 1951.

